

Final Report
GeoEngineers On-Call Agreement Y-7717
Task Order AU

**AN APPROACH FOR ESTIMATING INFILTRATION
RATES FOR STORMWATER INFILTRATION DRY
WELLS**

By
Joel Massmann, Ph.D., P.E.

Washington State Department of Transportation
Technical Monitor
Glorilyn Maw

Washington State Transportation Commission
Department of Transportation
and in cooperation with
U.S. Department of Transportation
Federal Highway Administration

April, 2004

DISCLAIMER

The contents of this report reflect the views of the author, who is responsible for the facts and the accuracy of the data presented herein. The contents do not necessarily reflect the official views or policies of the Washington State Transportation Commission, Department of Transportation, or the Federal Highway Administration. This report does not constitute a standard, specification, or regulation.

TABLE OF CONTENTS

1. Introduction and objectives.....	1
2. Description of drywell construction.....	1
3. Flow from drywells under transient conditions.....	2
4. Infiltration rates for drywells in various hydrogeologic systems.....	4
5. Equations for estimating steady-state infiltration rates.....	5
6. Comparisons between estimated and observed infiltration rates from dry wells.....	9
7. . Estimating draw-down times for dry wells.....	11
8. Recommendations for spacing of dry wells.....	13
9. Recommended design approach.....	13
ACKNOWLEDGMENTS	18
REFERENCES	18

APPENDICES

A	RESULTS OF COMPUTER SIMULATIONS WITH TRANSIENT, UNSATURATED MODEL
B	SUMMARY OF SPOKANE COUNTY DRYWELL TEST DATA
C	WATER LEVEL VERSUS TIME DATA FOR DRYWELLS

TABLES

<u>Table</u>		<u>Page</u>
1	Summary of geometry used to described double- and single-barrel dry wells	18
2	Unsaturated soil parameters.....	18
3	Infiltration rates and regression coefficients for different water table depths for the double-barrel configuration.....	19
4	Infiltration rates and gradient for different water table depths for the single-barrel configuration.....	20
5	Values assigned to the parameters used in the USBR and Hvorlsev equation	21
6	Comparison of infiltration rates with unsaturated model and various analytical solutions.....	21
7	Suggested analytical solutions for estimating infiltration from dry wells	22
8	Summary of results of field-scale dry well infiltration tests (unpublished data provided by J. Harakas, GeoEngineers, 2003).....	22
9	Summary of rates for water level declines during drywell infiltration tests (unpublished data provided by J. Harakas, GeoEngineers, 2003).....	23
10	Time required for the height of water to fall to 1% of their steady-state values for the double-barrel configuration.....	23

FIGURES

<u>Figure</u>		<u>Page</u>
1	Example of plans for pre-cast concrete drywells similar to what is used by the Washington State Department of Transportation (G. Maw, WSDOT, unpublished, 2004).....	24
2	Infiltration rate versus time for a typical dry well with a double-barrel geometry, hydraulic conductivity equal to 0.02 ft/minute, and depth to water 48 feet below the bottom of the drywell.....	25
3	Infiltrated volume versus time for the double-barrel geometry used in Figure 2.....	26
4	Infiltration rate versus volume infiltrated for the double-barrel geometry used in Figure 2.....	27
5	Approximations for describing infiltration rate versus volume infiltrated.	28
6	Regressions relating infiltration rates and depth to groundwater measured from below the bottom of the drywell.....	29
7	Results of regression equations 9) and 10) for estimating infiltration rate.	30
8	Observed drywell flow rates.....	31
9	Observed and calculated infiltration rates.....	32
10	Flow chart illustrating design approach.....	33

1. Introduction and objectives

This report describes an approach for estimating infiltration rates for dry wells that are constructed using standard configurations developed by the Washington State Department of Transportation. The approach was developed recognizing that the performance of these dry wells depends upon a combination of subsurface geology, groundwater conditions, and dry well geometry. The report focuses on dry wells located in unconsolidated geologic materials.

2. Description of drywell construction

Figure 1 illustrates an example of plans for pre-cast concrete drywells similar to what is used by the Washington State Department of Transportation (G. Maw, WSDOT, unpublished, 2004). The concrete cylinders used to construct the drywells are placed in excavations that are backfilled with gravel. The drywells are typically constructed with either one or two sections of seepage ports. The most common construction in Eastern Washington is the “double-barrel” construction in which two concrete sections are used. This is the construction shown on Figure 1. A “single-barrel” construction, which includes only one concrete section, is also used in some instances. Table 1 summarizes the geometry used in this study to describe the double- and single-barrel dry wells.

The excavation used in constructing a dry-well can be described as an inverted conical frustrum. The surface area of the sides and bottom of this excavation is given by the following expression (Beyer, 1987):

$$Area = \pi(R_1 + R_2)\sqrt{(R_1 - R_2)^2 + h^2} + \pi R_2^2 \quad (1)$$

where R_1 is the radius at the ground surface, R_2 is the radius at bottom of the excavation, and h is the depth of the excavation. Surface areas calculated with Equation 1 for single- and double-barrel drywells are included in Table 1. Table 1 also gives the radius for a right-circular cylinder with bottom and side area equal to the bottom and side area of the

inverted conical frustrum. This equivalent radius will be used in subsequent sections with equations that describe flow from boreholes.

3. Flow from drywells under transient conditions

Flow from drywells under transient conditions can be described with the 2-dimensional saturated-unsaturated finite-difference model VS2DH 3.0 (Hsieh et al., 2000). This model, which is described in more detail in Massmann (2003a), can be used to simulate radial flow systems similar to what would be developed in the vicinity of drywells. Figure 2 presents example results for a dry well with a double-barrel geometry at a site where the depth to groundwater is 48 feet below the bottom of the drywell and the saturated hydraulic conductivity is 0.02 feet per minute. (It should be noted that the convention used in this report is to define depth as the distance below the bottom of the drywell and not the depth below the land surface.) The unsaturated soil parameters were defined using the van Genuchten equation (van Genuchten, 1980). The vertical axis gives infiltration rate in cubic feet per second (cfs) and the horizontal axis is time in minutes. Figure 2 shows the typical response for flow in unsaturated systems where the infiltration rate decreases with time as the wetting front moves downward and eventually reaches a steady-state rate. (The somewhat jagged appearance of the curve during early times is a numerical artifact caused by the grid cells used to discretize the flow field.) For the geometry and soil properties used in the example shown in Figure 2, the steady-state infiltration rate is approximately 0.45 cfs and occurs after approximately 200 minutes. It should be noted that the early-time infiltration rate is significantly higher than this steady-state value.

Figure 3 shows the total volume of water that has been infiltrated as a function of time. This curve is derived by integrating the rate-versus-time curve shown in Figure 2. The curve – plotted on logarithmic scales – is approximately linear. Approximately 1,000 cubic feet of water is infiltrated after 20 minutes and approximately 10,000 cubic feet is infiltrated after 200 minutes. (As a reference point, the runoff from a one-acre paved site with 1 inch of rainfall is 3,630 cubic feet.)

The results presented in Figures 2 and 3 can be combined to develop a relationship between infiltration rate and the volume of water that has been infiltrated. This format for presenting the data will be useful for comparing performances of systems with different hydraulic conductivity values and will be used in the design approach described below. Figure 4 shows the infiltration rate versus infiltrated volume for the example drywell. This curve can be approximated with two straight lines on logarithmic scales, as shown in Figure 5. The first line describes the transient portion of the infiltration process and the second horizontal line describes the steady-state infiltration rate. The transient curve can be described using the following power-law expression:

$$Q = aV^b \quad (2)$$

where Q is the infiltration rate in cfs, V is the volume infiltrated in cubic feet, and “ a ” and “ b ” are coefficients. For the example shown in Figure 5, the “ a ” coefficient is equal to 3.8 and the “ b ” coefficient is equal to -0.29 . The second horizontal line describes the steady-state part of the curve and is given by the following expression:

$$Q = c \quad (3)$$

where “ c ” is the steady-state infiltration rate. This steady-state rate is approximately 0.45 cfs for the example shown in Figure 5.

The point on the horizontal axis (the volume axis) where these two straight lines intersect, V^* , is given by the following equation:

$$V^* = e^{\frac{\ln(c/a)}{b}} \quad (4)$$

The parameters a , b , c , and V^* will be used to describe the infiltration rate versus volume curves.

4. Infiltration rates for drywells in various hydrogeologic systems

The VS2DH 3.0 model referenced above was used to estimate infiltration rates for single- and double-barrel dry wells in various hydrogeologic systems. These hydrogeologic systems were defined in terms of the depth to groundwater and the hydraulic conductivity of the unsaturated or vadose zone. The depth of water below the bottom of the drywell ranged from 3 feet to 48 feet and the hydraulic conductivity values ranged from 0.005 ft/min to 0.20 ft/min. This range of hydraulic conductivity was selected because it results in discharge rates in the range of 0.1 to 10 cfs. This covers the range of typical field values. The water level in the dry well was held at a constant level equal to elevation of the ground surface. The unsaturated hydraulic characteristics were represented by the van Genuchten equation (van Genuchten, 1980):

$$\theta = \frac{\theta_s - \theta_r}{[1 + (\alpha|\psi|)^\beta]^{1-\frac{1}{\beta}}} \quad (5)$$

Where θ is the volumetric moisture content (dimensionless), θ_r is the residual moisture content (dimensionless), θ_s is the saturated moisture content (dimensionless), ψ is the suction head (L), α is the van Genuchten alpha parameter (L^{-1}), and β is the van Genuchten beta parameter (dimensionless). Table 2 gives values for these parameters. These values were held constant in all simulations. It should be noted that the van Genuchten parameters are included in the report for completeness and full documentation of the computer model used to estimate the infiltration rates. Estimates of steady-state infiltration rates from drywells are insensitive to these parameters and these parameters are not required for the design equations that are presented in subsequent sections.

Appendix A gives the results of the computer simulations in terms of infiltration rate as a function of volume of water infiltrated. These results are summarized in Tables 3 and 4. Table 3 gives steady-state infiltration rates for double-barrel configurations. The power-law coefficients given in Table 3 (a, b, and V^*) were defined in the previous

section. The lines used to define these power-law coefficients are included with the results in Appendix A. Steady-state rates and power-law coefficients for single-barrel configurations are included in Table 4.

The combinations of water table depths and hydraulic conductivity values resulted in infiltration rates that ranged from more than 5 cfs to less than 0.1 cfs. The results show that the infiltration rates are linearly proportional to the hydraulic conductivity value if the depth to the water table is fixed (e.g., the infiltration rate for a hydraulic conductivity of 0.2 ft/minute is ten times larger than the infiltration rate for a hydraulic conductivity of 0.02 ft/minute for all simulations). These results also show that as the depth to the groundwater decreases, the steady-state infiltration rate also decreases. This effect is most pronounced if the depth to the water table is less than 30 feet below the bottom of the drywell. The simulations suggest that if the depth to the groundwater table is greater than 30 feet, the water table has little effect on the steady-state infiltration rate. A comparison of Tables 3 and 4 shows that the double barrel rates are between 1.5 and 2 times larger than the single-barrel rates.

The values for V^* included in Tables 3 and 4 are somewhat counter-intuitive in that simulations on systems with shallow water tables give larger values than simulations on systems with deep water tables. The V^* values can be interpreted as the volume of water that must be infiltrated before infiltration rates become steady or nearly constant with time. For shallow water tables, the infiltration rates do not approach steady-state values until a groundwater mound has formed beneath the facility. For deep water tables, the infiltration rates approach steady-state before the groundwater mounds form because the deeper water table allows the wetting front to move deep enough for the gradient to approach 1 (as described in Massmann, 2003a).

5. Equations for estimating steady-state infiltration rates

Several analytical solutions are available for estimating discharge from boreholes. These solutions can be adopted to estimate infiltration rates from dry wells. Estimates of infiltration rates from the unsaturated flow models described earlier were compared to

estimates derived from three analytical solutions to evaluate the magnitude of error associated with predictions from the more simplified approaches.

The following three analytical solutions were compared: 1) the U.S. Bureau of Reclamation (USBR) solution, 2) the Hvorslev solution for deep flow fields, and 3) the Hvorslev solution for shallow flow fields. All three of these solutions are empirically-derived equations that were originally developed to describe flow from boreholes or wells. The USBR solution (Equation 6 below) is described in U.S. Department of Interior (1990) and was developed specifically for open boreholes (boreholes without well screens or casings) located above the water table. The Hvorslev solutions for deep and shallow flow fields (Equation 7 and 8 below, respectively) are described in Lambe and Whitman (1979) and were developed for well points in saturated systems.

The USBR solution:

$$Q = \frac{2\pi KH^2}{\ln\left[\frac{H}{r} + \sqrt{1 + \left(\frac{H}{r}\right)^2}\right] - \frac{\sqrt{1 + (H/r)^2}}{H/r} + \frac{1}{H/r}} \quad (6)$$

where Q is the discharge rate (L³/t), K is the saturated hydraulic conductivity value (L/t), H is the height of water in the borehole (L), r is the radius of the borehole (L).

The Hvorslev deep flow field solution:

$$Q = \frac{2\pi KLH}{\ln\left[\frac{2L}{r} + \sqrt{1 + \left(\frac{2L}{r}\right)^2}\right]} \quad (7)$$

The Hvorslev shallow flow field solution:

$$Q = \frac{2\pi K L H}{\ln \left[\frac{4L}{r} + \sqrt{1 + \left(\frac{4L}{r} \right)^2} \right]} \quad (8)$$

where Q is the discharge rate (L^3/t), K is the saturated hydraulic conductivity value (L/t), H is the height of water in the well (L), L is the length of the screen portion of the well (L), r is the radius of the well (L).

The values assigned to the parameters used in the USBR and Hvorslev equations to simulate flow from a dry well are described in Table 5. Table 6 compares the results from the analytical solutions with the estimates from the unsaturated model described above. This comparison is provided for the deep water table (depth to groundwater equal to 48 feet) and the shallow groundwater table (depth to groundwater equal to 3 feet) cases for both double-barrel and single-barrel configurations. For the deep water table case, the USBR and Hvorslev deep flow field solutions both give results that are relatively close to the values from the unsaturated model. Both solutions are conservative in that they under-estimate the flow relative to the unsaturated model, with the Hvorslev solution giving slightly lower values.

For the shallow water table case, the USBR solution over-estimates flow for both double-barrel and single-barrel configurations. The Hvorslev deep flow field solution overestimates flows for the double barrel configuration but gives reasonably close values for the single-barrel configuration, when applied to the shallow water table case. The Hvorslev shallow flow field solution under-estimates flows for both single and double-barrel configurations.

Table 7 gives suggested analytical solutions based on the comparisons included in Table 6. For single-barrel configurations with shallow water tables, both the Hvorslev deep and the Hvorslev shallow solutions underestimate flow relative to the computer simulations. Intermediate values between those calculated using the two Hvorslev solutions may be appropriate in these cases.

The results of the computer simulations included in Tables 3 and 4 can also be used to develop regression equations relating steady-state flow rates with saturated hydraulic conductivity values and the depth to groundwater. The following two regression equations were derived from the results in Tables 3 and 4.

$$\text{Double barrel wells:} \quad Q = K[3.55\ln(D_{wt}) + 12.32] \quad (9)$$

$$\text{Single barrel wells:} \quad Q = K[1.34\ln(D_{wt}) + 8.81] \quad (10)$$

Where Q is the infiltration rate in cfs, K is the saturated hydraulic conductivity value in ft/minute, and D_{wt} is the depth from the bottom of the drywell to groundwater in feet. The regressions given by equations (9) and (10) are shown in Figure 6. Figure 7 shows how these regressions match the data in Tables 3 and 4.

The estimated infiltration rates given by equations 9 and 10 represent steady-state values. If the maximum volume or design volume of water that must be infiltrated is significantly less than the V^* values included in Tables 3 and 4, then the average infiltration rate during the event may be significantly larger than the steady-state values. Using equations 9) and 10) to design dry wells provides a level of conservatism because of the higher infiltration rates that occur during the early transient part of the infiltration event. If the “design” rainfall runoff events are expected to occur rarely, then it may be reasonable to assume that a significant portion of the water may infiltrate during the transient part of the curves that are shown in Figures 2 and 4.

The power-law expressions described in Tables 3 and 4 can be used to estimate an infiltration rate for different runoff volumes using equation 2:

$$Q = aV^b \quad (2)$$

where the coefficients “a” and “b” are given in Tables 3 and 4 and the volume of the run, V , is given in cubic feet. The flow rate in Equation 2, Q , is given in cfs. A comparison of this transient infiltration rate to the steady-state rates given by Equations 9) and 10) will provide a measure of the conservatism inherent in using the steady-state values.

6. Comparisons between estimated and observed infiltration rates from dry wells

The results of field measurements of infiltration rates from dry wells in Eastern Washington are included in Appendix B. These data were collected and compiled by GeoEngineers as part of their ongoing project with the City of Spokane (need reference for this). The data that are included in Appendix B were selected because they represent sites where estimates of hydraulic conductivity were available, as well as measured values of flow rates and water levels in the dry wells. Table 8 summarizes the data in terms of estimated hydraulic conductivity and observed dry well infiltration rates. The hydraulic conductivity estimates included in Table 8 were derived by taking the geometric mean of the data that were collected at each site. At sites where only a single estimate for hydraulic conductivity was available, the geometric mean is equal to the observed value.

The relationship between the geometric mean of the hydraulic conductivity and the observed infiltration rate from the dry wells is shown in Figure 8. This figure shows that while the estimated hydraulic conductivity values range over approximately 3 orders of magnitude, the observed infiltration rates are in the range of 0.2 to 2 cfs. The apparent insensitivity of the flow rates to the estimated hydraulic conductivity is likely due to spatial variability and measurement error. Most of the hydraulic conductivity values were estimated from grain size information using the Hazen equation (discussed below and described in Massmann, 2003b). The Hazen equation and other equations based on grain-size relationships give order-of-magnitude estimates of hydraulic conductivity. These values also represent estimates over relatively small areas or volumes. Infiltration from the dry wells will be dependent upon the hydraulic conductivity over a much larger area or volume. Furthermore, the flow from the dry

wells will tend to be controlled by the higher conductivity areas intercepted by the dry well.

Table 8 also includes estimates of infiltration rates based on the USBR equation described above (Equation 6). A comparison of these estimates with observed flow rates is provided in Figure 9. Equation (6) was used because it allows infiltration estimates to be developed as a function of the height of water in the dry well. In most of the dry well tests described in Table 8 and Appendix B, the dry well was not full. In general, the estimated infiltration rate from the USBR equation is less than the observed rate from the field tests. Again, this difference is likely due to the spatial variability and measurement error in the hydraulic conductivity values. All of the models described earlier (the unsaturated model, the USBR equation, and the two Hvorslev equations) show that infiltration rates are linearly-dependent upon hydraulic conductivity value. The flows should be directly proportional to the hydraulic conductivity values.

It should be noted that the estimates of infiltration rates developed using the computer simulations and included in Tables 3 and 4 represent maximum values that would result when the dry well is completely filled with water. This was not the condition for most of the dry well tests described in Appendix B. It is not meaningful to compare the field data with the regression equations because of this difference in assumed and actual water levels. The USBR equation and the computer model or regression equation give very similar estimates for dry wells that are full, as demonstrated from the results included in Table 6. The regressions equations were developed to provide an easy-to-use and convenient approach to estimate the maximum infiltration rates for drywells. These equations were not developed to evaluate field data.

The lack of proportionality in the results included in Figure 9 suggest that the geometric mean of the hydraulic conductivity values from the grain size curves underestimate the effective hydraulic conductivity for the dry wells. This results in conservative estimates for infiltration from dry wells. Comparisons were also made using the maximum hydraulic conductivity at each site (rather than the geometric mean

included in Table 8). This approach gave a slightly better fit between estimated and observed infiltration rates, but the observed infiltration rates were generally still higher than the estimated rates. (It should be noted that at most of the sites included in Table 8, only a single estimate of hydraulic conductivity was available and so the geometric mean is the same as the maximum value. In general, geometric mean values will provide more reliable estimates of infiltration rates than maximum values.)

7. Estimating draw-down times for dry wells

As part of several of the drywell tests summarized in Appendix B, rates of water level declines were monitored after the inflow to the drywells had been shut off. The results of these “falling-head” tests are described in Table 9. The hydraulic conductivity values given in the second column of Table 9 are based on the steady-state flow rates that were observed during the dry well tests. These values were derived by using the USBR equation (Equation 6) to calculate the hydraulic conductivity corresponding to the observed flow rate and water level during steady conditions. The fourth column in Table 9 gives the height of water in the dry well at the end of the steady-state portion of the test and at the beginning of the falling-head portion of the test. The fifth column gives the observed time for the height of water in the well to decline to a value equal to one-half of the initial, steady-state value. The last two columns give the height of water and the time at the end of the test.

The data shown in Table 9 show that water level decline occurs relatively quickly in these test wells. These observations are consistent with the rate of water level declines that are predicted using Hvorslev equations for falling head tests in well points (Lambe and Whitman, 1979). The following two equations can be used to estimate the rate of water level declines that correspond to the Hvorslev equations for deep and shallow flow fields (Equations 7 and 8 given above):

$$t_2 - t_1 = \ln \left[\frac{2L}{r} + \sqrt{1 + \left(\frac{2L}{r} \right)^2} \right] \frac{r^2}{2LK} \ln \left(\frac{H_1}{H_2} \right) \quad (11)$$

where K is the saturated hydraulic conductivity value (L/t), H_1 and H_2 are the height of water in the well (L) at times t_1 and t_2 , L is the length of the screen portion of the well (L), and r is the radius of the well (L). Although this equation was developed for saturated systems, the comparisons between the Hvorslev equation and the unsaturated model described earlier suggest that it will provide reasonable estimates for drywell performance. Table 10 gives the times required for the height of water in the drywells to fall to 1% of their steady-state values for the double-barrel configuration. Although it should be noted that the Hvorslev equation was developed for well points in saturated systems, the results in Table 10 suggest that dry wells with infiltration rates in the range of 0.1 to 1 cfs will likely drain within the 72-hour (4,320 minute) period that is recommended or required by some regulatory agencies.

The times for water level declines given in Tables 9 and 10 reflect the time for the water to drain from the drywells. It is important to recognize that groundwater mounds that form beneath drywells will likely take much longer to dissipate – perhaps on the order of weeks or months depending upon the volume of water that was infiltrated and site-specific hydrogeological characteristics. An infiltration event that begins before the groundwater mound has fully dissipated will cause steady-state conditions to be achieved more quickly than the case with no initial mound or mound remnant. Because the steady-state infiltration rate is less than the transient rate (as described in Figures 2 and 4), the net effect of the residual mound will be a reduction in average infiltration rate, as compared to the case with no initial mound.

The estimated infiltration rates given in Tables 3 and 4 include the effects of groundwater mounding. The regression equations that were developed based on these results (Equations 9 and 10) also include these effects. Tables 6 and 7 describe when the Hvorslev and USBR equations are conservative, relative to the regression equations and the results of the computer simulations. Provided that the regression equations are used or that the recommendations included in Table 7 are used for the Hvorslev or USBR equations, the “correction factor” for mounding is built into the analysis and is not required.

8. Recommendations for spacing of dry wells.

The results of the unsaturated flow models described earlier can be used to suggest well spacing for sites with multiple dry wells. In general, sites with lower hydraulic conductivity values and sites with more shallow water tables will require greater spacing than sites with high hydraulic conductivity values and deep water tables. For sites with water tables greater than 30 feet, the recommended spacing to prevent overlap of groundwater mounds is 5 times the radius of the excavation for the dry well, or approximately 50 feet. (This spacing is defined as the distance from center point to center point for the wells.) For sites with water tables less than 10 feet, the recommended spacing is 8 times the radius of the dry well or approximately 80 feet. Dry wells spaced more closely than these recommended rates may still be effective, but it should be noted that there could be some reduction in infiltration rates caused by overlapping mounds. The regression equations and the results in Tables 3 and 4 were developed assuming no overlap between mounds from adjacent drywells. If wells are spaced more closely than the values described above, the design engineer should be aware that there could be some reduction in infiltration rates as compared to the single-well scenario used to develop the regression equations.

9. Recommended design approach

A flow chart with the recommended design approach is included as Figure 10. The steps included in this chart are described in the sections that follow.

9.1 Perform subsurface site characterization and data collection.

As a minimum, these site characterization activities should be used to define subsurface layering and the depth to groundwater and to collect samples for grain size analyses (Massmann 2003b). Samples should be collected from each layer beneath the facility to the depth of groundwater or to approximately 40 feet below the ground surface (approximately 30 feet below the base of the drywell).

9.2 Estimate saturated hydraulic conductivity from soil information, laboratory tests, or field measurements

A variety of methods can be used to estimate saturated hydraulic conductivity. These methods include estimates based on grain size information, laboratory permeameter tests, air conductivity measurements, infiltrometer tests, and pilot infiltration tests. Advantages and disadvantages of these various methods are described in Massmann (2003b).

Preliminary estimates may be derived using grain size information, as described in Massmann (2003b). Two approaches include the Hazen equation and the log-based regression. The Hazen equation is given as follows:

$$K_{sat} = CD_{10}^2 \quad (12)$$

where K_{sat} is the saturated hydraulic conductivity, C is a conversion coefficient, and D_{10} is the grain size for which 10% of the sample is more fine (10% of the soil particles have grain diameters smaller than D_{10}). For K_{sat} in units of cm/s and for D_{10} in units of mm, the coefficient, C , is approximately 1.

A second approach for estimating saturated hydraulic conductivities for soils was proposed by Massmann (2003b):

$$\log_{10}(K_{sat}) = -1.57 + 1.90D_{10} + 0.015D_{60} - 0.013D_{90} - 2.08f_{fines} \quad (13)$$

where D_{60} and D_{90} are the grain sizes for which 60% and 90% of the sample is more fine and f_{fines} is the fraction of the soil (by weight) that passes the number-200 sieve. This approach is based on a comparison of hydraulic conductivity estimates from air permeability tests with grain size characteristics. Other regression relationships between saturated hydraulic conductivity and grain size distributions are available, as described in Massmann (2003b).

It should be noted that the estimates given above should be viewed as “order-of-magnitude” estimates. If measurements of hydraulic conductivity are available from laboratory or field tests (as described below), these data should be weighed more heavily in selecting values of hydraulic conductivity for design purposes.

9.3 Calculate geometric mean values for sites with multiple hydraulic conductivity values.

The geometric mean for hydraulic conductivity value is given by the following expressions:

$$K_{\text{geometric}} = e^{Y_{\text{average}}} \quad (14)$$

where Y_{average} is the average of the natural logarithms of the hydraulic conductivity values:

$$Y_{\text{average}} = \frac{1}{n} \sum Y_i = \frac{1}{n} \sum \ln(K_i) \quad (15)$$

9.4 Estimate the uncorrected, steady-state infiltration rate for the dry wells

Uncorrected steady-state infiltration rates for single- and double-barrel configurations can be estimated using the regression equations given by Equations 9 and 10. The values from the regression equation can be compared with the results in Tables 3 and 4 to ensure that there have not been errors in the calculation. The results derived using Equations 9 and 10 should be in the range of the values included in Tables 3 and 4.

9.5 Estimate the volume of stormwater and the stormwater inflow rates that must be infiltrated by the proposed or planned drywell.

The volume of stormwater that must be infiltrated and the rate at which this must occur are generally specified by local, regional, or state requirements. In many cases, the volume and required rates of discharge are controlled by both water quality and water quantity concerns. The volume of storm water that must be infiltrated can be estimated using the approaches summarized in Massmann (2003b).

9.6 Apply corrections for siltation

Although the comparison of calculated and observed infiltration rates shown in Figure 9 suggests that using the geometric mean of hydraulic conductivity values will generally result in conservative designs, it should be noted that these data were collected from relatively new dry wells. Siltation and plugging may reduce the equivalent hydraulic conductivity values of the facilities by an order of magnitude or more. This will result in a corresponding reduction in infiltration rate, as shown in Tables 3 and 4. If pre-treatment cannot be provided, the design infiltration rates calculated in Section 9.4 should be reduced by a factor on the order of 0.5 or less.

9.7 Monitor performance after construction.

Full-scale tests should be conducted at all sites on a periodic basis where possible. If a source of water is available (e.g. nearby fire hydrants or water trucks), these tests should be conducted using controlled and measured inflow rates. If water sources are not available, inflow rates should be monitored if at all possible. By monitoring inflow rates, relationships can be developed that give infiltration rates as a function of stage or water level in the dry well. These can be compared to the values estimated using the computer model or the analytical solutions.

In cases where the full-scale tests indicate infiltration rates that are significantly less than the design rates, the facility may need to be modified. If the lower rates are expected to be caused by soil plugging, then remediation of the existing dry well may be possible. For some sites, particularly those where the lower rates are due to unexpectedly high groundwater levels, there may be little that can be done.

ACKNOWLEDGMENTS

The author wishes to acknowledge the generous help and support provided during the study by Glorilyn Maw, Tony Allen, and Greg Lahti at the Washington State Department of Transportation and by Jim Harakas at GeoEngineers for sharing their drywell field data and experiences.

REFERENCES

- Beyer, W.H. (editor), *CRC Standard Mathematical Tables*, CRC Press, Boca Raton, Florida, 1987.
- Lambe, T.W. and R.V. Whitman, *Soil Mechanics*, SI version, John Wiley, New York, 1979.
- Massmann, J., *Implementation of Infiltration Ponds Research*, WA-RD 578.1, October 2003a.
- Massmann, J., *A Design Manual for Sizing Infiltration Ponds*, WA-RD 578.2, October 2003b
- U.S. Department of the Interior, "Procedure for Performing Field Permeability Testing by the Well Permeameter Method (USBR 7300-89)," in *Earth Manual, Part 2, A* Water Resources Technical Publication, 3rd ed., Bureau of Reclamation, Denver, Colo., 1990.

Table 1 – Summary of geometry used to described double- and single-barrel dry wells.

	Dry well construction	
	Double barrel	Single barrel
Excavation depth (ft)	12	8
Radius of bottom of excavation (ft)	4	3
Radius of top of excavation (ft)	10	8
Surface area of gravel-backfilled section (ft ²)	500	250
Equivalent radius of right circular cylinder (ft)	7.1	5.7

Table 2— Unsaturated soil parameters

Parameter	Value
Saturated moisture content (θ_s)	0.25
Residual moisture content (θ_r)	0.075
α (ft⁻¹)	7.5
α (cm⁻¹)	0.25
β (dimensionless)	1.9

Table 3—Infiltration rates and regression coefficients for different water table depths for the double-barrel configuration

Depth of water table (ft)	Hydraulic conductivity beneath facility (ft/min)	Steady-state infiltration rate (cfs)	Power law coefficients		
			a	b	V*
3	0.005	0.084	0.44	-0.1903	6014
	0.02	0.32	1.98	-0.2015	8475
	0.05	0.81	5.21	-0.2076	7831
	0.10	1.62	11.2	-0.2173	7316
	0.20	3.24	24.3	-0.2296	6475
8	0.005	0.097	0.49	-0.1808	7774
	0.02	0.39	2.05	-0.1829	8717
	0.05	0.976	5.13	-0.1825	8889
	0.10	1.95	10.7	-0.1829	11025
	0.20	3.89	22.2	-0.1936	8073
28	0.005	0.125	0.52	-0.1722	3937
	0.02	0.50	1.99	-0.1670	3909
	0.05	1.25	4.84	-0.1649	3676
	0.10	2.50	9.25	-0.1582	3905
	0.20	5.00	18.4	-0.1577	3874
48	0.005	0.127	0.52	-0.1770	2876
	0.02	0.51	1.97	-0.1683	3070
	0.05	1.27	4.71	-0.1621	3247
	0.10	2.55	9.30	-0.1602	3219
	0.20	5.10	18.6	-0.1598	3285

Table 4—Infiltration rates and gradient for different water table depths for the single-barrel configuration

Depth of water table (ft)	Hydraulic conductivity beneath facility (ft/min)	Steady-state infiltration rate (cfs)	Power law coefficients		
			a	b	V*
3	0.005	0.051	0.20	-0.1590	5401
	0.02	0.20	0.81	-0.1619	5650
	0.05	0.51	2.16	-0.1721	4391
	0.10	1.02	4.34	-0.1743	4056
	0.20	2.04	8.91	-0.1780	3953
8	0.005	0.058	0.20	-0.1477	4363
	0.02	0.23	0.81	-0.1502	4367
	0.05	0.59	2.03	-0.1512	3542
	0.10	1.18	4.09	-0.1534	3305
	0.20	2.34	8.02	-0.1509	3508
28	0.005	0.068	0.26	-0.1917	1092
	0.02	0.27	0.94	-0.1736	1321
	0.05	0.68	2.18	-0.1622	1316
	0.10	1.35	4.23	-0.1583	1359
	0.20	2.70	8.10	-0.1509	1452
48	0.005	0.068	0.25	-0.1864	1080
	0.02	0.28	0.88	-0.1650	1033
	0.05	0.69	2.06	-0.1543	1198
	0.10	1.36	3.97	-0.1482	1378
	0.20	2.72	7.80	-0.1455	1395

Table 5 – Values assigned to the parameters used in the USBR and Hvorslev equations

	USBR Solution		Hvorslev solutions	
	Double-barrel	Single-barrel	Double-barrel	Single-barrel
L (ft)	Not applicable	Not applicable	8	4
H (ft)	12	8	12	8
r (ft)	7.1	5.7	7.1	5.7

Table 6—Comparison of infiltration rates with unsaturated model and various analytical solutions.

Dry well Geometry	Hydraulic conductivity beneath facility (ft/min)	Steady-state infiltration rate from unsaturated model (cfs)	Analytical solutions		
			USBR solution for bore holes	Hvorslev deep flow field	Hvorslev shallow flow field
Double Barrel, water table at 3 feet	0.005	0.084	0.10	0.094	0.052
	0.02	0.32	0.42	0.37	0.21
	0.05	0.81	1.04	0.94	0.52
	0.10	1.62	2.08	1.87	1.04
	0.20	3.24	4.16	3.74	2.08
Double Barrel, water table at 48 feet	0.005	0.127	0.10	0.094	0.052
	0.02	0.51	0.42	0.37	0.21
	0.05	1.27	1.04	0.94	0.52
	0.10	2.55	2.08	1.87	1.04
	0.20	5.10	4.16	3.74	2.08
Single Barrel, water table at 3 feet	0.005	0.051	0.065	0.049	0.026
	0.02	0.20	0.26	0.20	0.10
	0.05	0.51	0.65	0.49	0.26
	0.10	1.02	1.29	0.97	0.51
	0.20	2.04	2.58	1.95	1.02
Single Barrel, water table at 48 feet	0.005	0.068	0.065	0.049	0.026
	0.02	0.28	0.26	0.20	0.10
	0.05	0.69	0.65	0.49	0.26
	0.10	1.36	1.29	0.97	0.51
	0.20	2.72	2.58	1.95	1.02

Table 7 –Suggested analytical solutions for estimating infiltration from dry wells.

Solution	Deep water table (>35 feet)		Shallow water table (<35 feet)	
	Double-barrel	Single-barrel	Double-barrel	Single-barrel
USBR	Yes	Yes	No	No
Hvorslev deep	Yes	Yes	No	Yes
Hvorslev shallow	No	No	Yes	Yes

Table 8 – Summary of results of field-scale dry well infiltration tests (unpublished data provided by J. Harakas, GeoEngineers, 2003)

Site	Hydraulic conductivity estimates				Dry well flow rates (cfs)		
	Grain Size	Test Pits	Bore hole	Geometric mean	Observed	USBR Equation	Relative Error
NW Tech Park	4	1		8.3E-04	0.568	0.08	86%
Hayford Plaza	4	1		5.9E-03	0.62	1.84	-197%
Shady Slope	3	2		1.3E-03	0.81	0.16	80%
Trickle Creek	1			1.6E-05	0.086	0.01	93%
Summer Crest	2			8.9E-05	0.52	0.04	93%
Midway A	1			1.1E-04	0.03	0.03	-14%
Midway B	1			1.1E-03	0.51	0.96	-87%
Mt. Spokane 1			1	4.6E-04	1.32	0.20	85%
Mt. Spokane 3			1	3.6E-04	1.17	0.15	87%
Westwood N. DW-2	1			2.0E-03	1.5	1.48	2%
Westwood N. DW-3	1			2.9E-03	1.42	1.75	-23%
Westwood N. DW-6	1			1.9E-03	1.11	0.12	89%
Westwood N. DW-7	1			6.1E-04	1.44	1.12	22%
Westwood N. DW-8	1			2.3E-03	0.9	0.92	-3%
Westwood N. DW-9	1			1.3E-04	0.62	0.04	94%
Westwood N. DW-10	1			4.2E-03	0.38	0.76	-100%
Westwood N. DW-12	1			3.4E-04	0.95	0.29	69%
Westwood N. DW-14	1			6.1E-04	0.79	0.54	32%
Westwood N. DW-15	1			6.1E-04	0.74	0.54	27%
Westwood N. DW-20	1			3.8E-05	0.87	0.03	96%
5 Mile Prairie	1			2.3E-03	1.31	1.93	-47%
Dartford	1			6.9E-04	0.28	0.66	-136%
Dartford	1			1.9E-04	0.26	0.07	73%
5 Mile Prairie	1			1.4E-03	0.22	0.84	-283%
5 Mile Prairie	1			4.6E-04	0.27	0.33	-23%
5 Mile Prairie			1	2.3E-05	0.29	0.02	92%
5 Mile Prairie			1	2.3E-04	0.58	0.25	57%

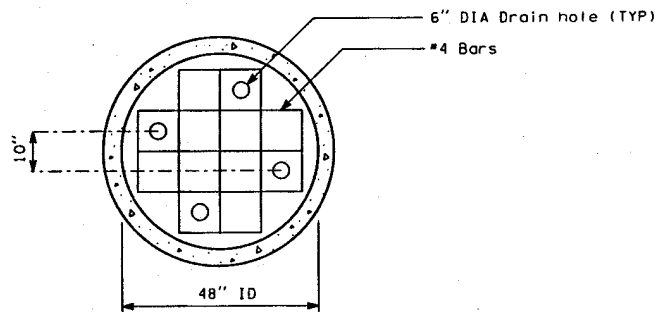
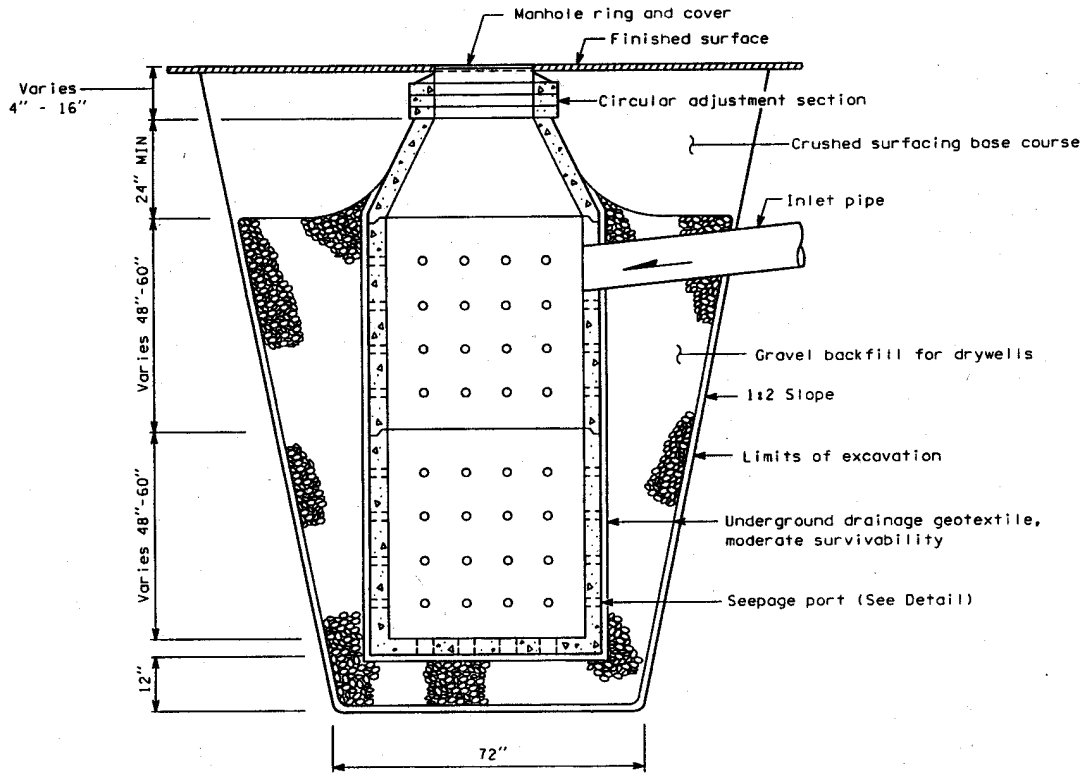
Table 9 – Summary of rates for water level declines during drywell infiltration tests
(unpublished data provided by J. Harakas, GeoEngineers, 2003)

Site	Hydraulic conductivity (ft/min)	Steady-state flow rate (cfs)	Height of water at beginning of test (ft)	Time for height of water to reduce by one-half (minutes)	Height of water at end of test (ft)	Time for end of test (minutes)
Hayford Plaza	0.29	0.62	4.2	15.0	0.07	149
NW Technology Park	1.46	0.56	0.94	21.5	0.34	38.5
Trickle Creek	0.03	0.09	4.75	64	1.0	142.0
Summer Crest	0.17	0.52	5.5	4.0	0.1	28.0

Table 10 - Time required for the height of water to fall to 1% of their steady-state values for the double-barrel configuration

K (ft/min)	Steady-state infiltration rate from Equation 7 (cfs)	Time for $H_2/H_1=0.01$ from Equation 11 (minutes)
0.005	0.1	3900
0.02	0.4	1000
0.05	1	400
0.1	2	200
0.2	4	100

Figure 1



BASE DETAIL

Figure 2

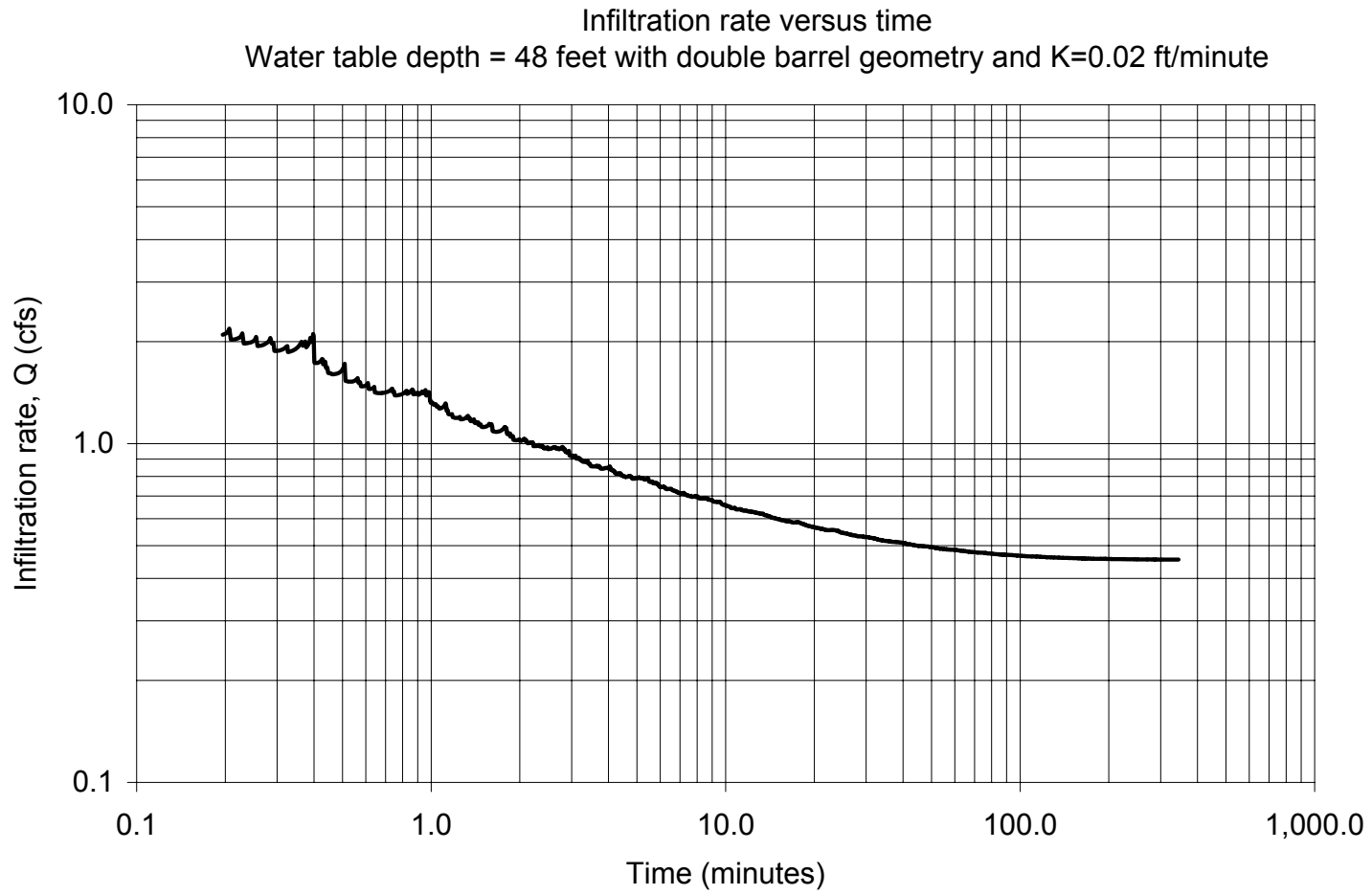


Figure 3

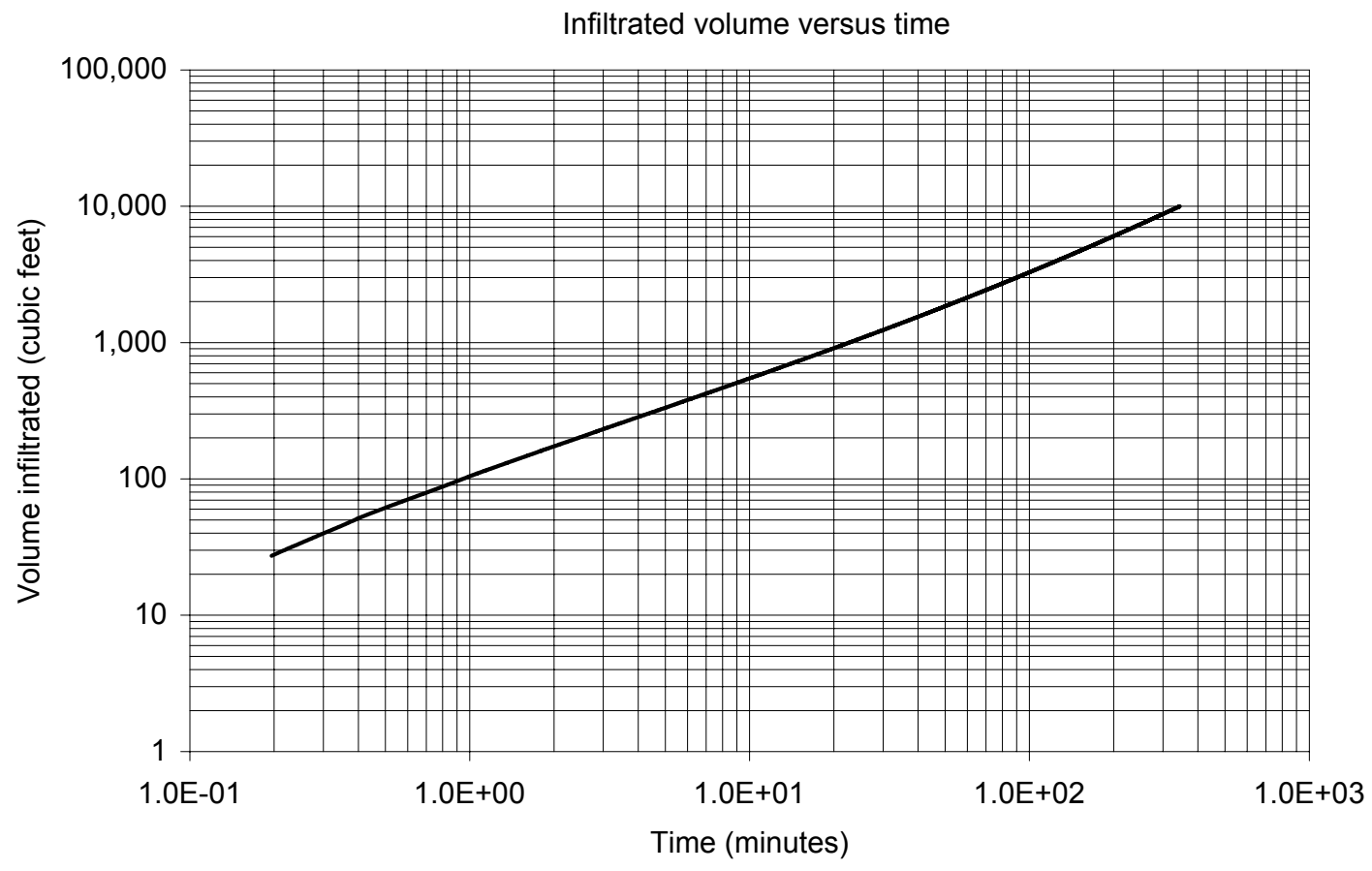


Figure 4

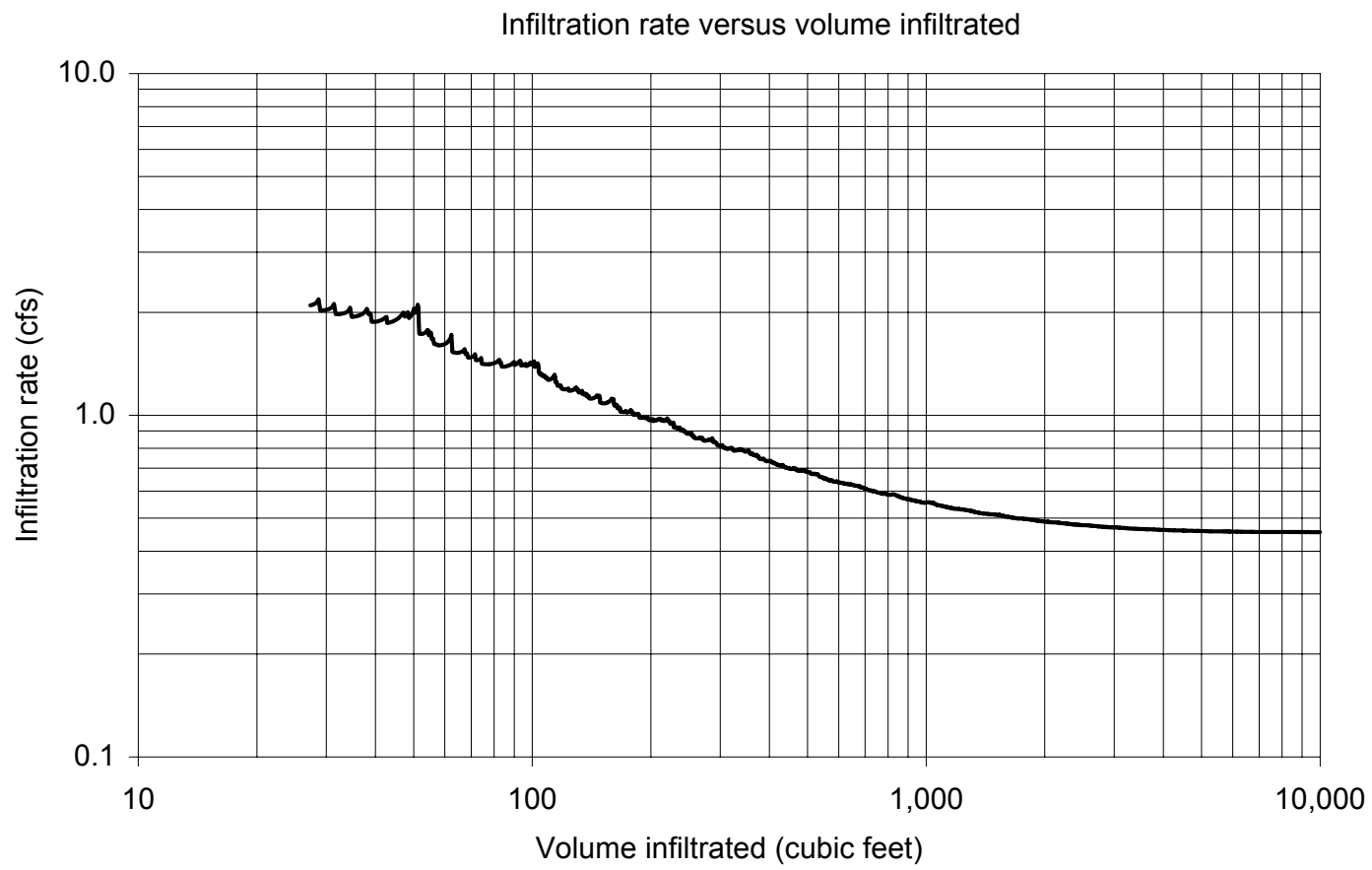


Figure 5

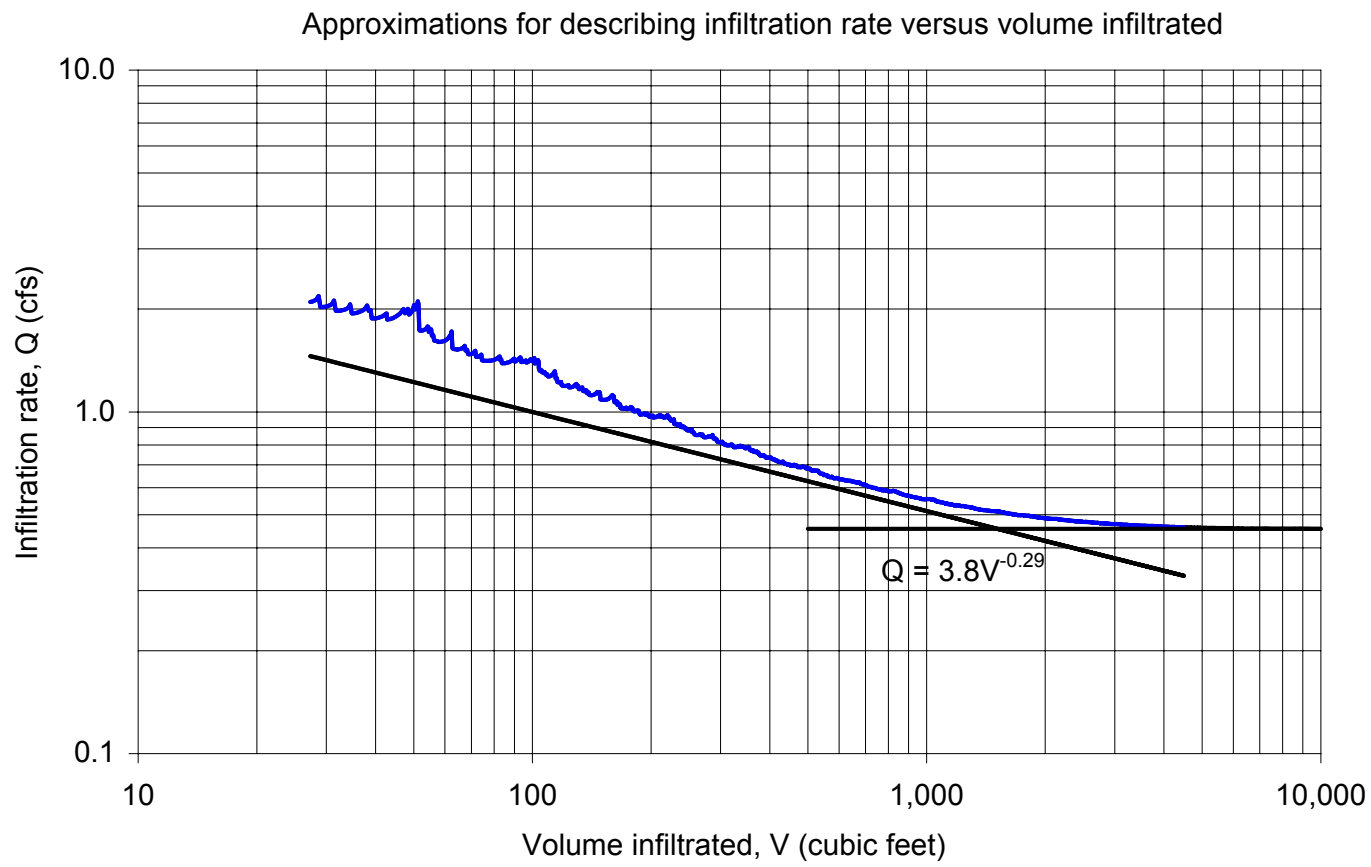


Figure 6

Regressions relating infiltration rates and depth to groundwater

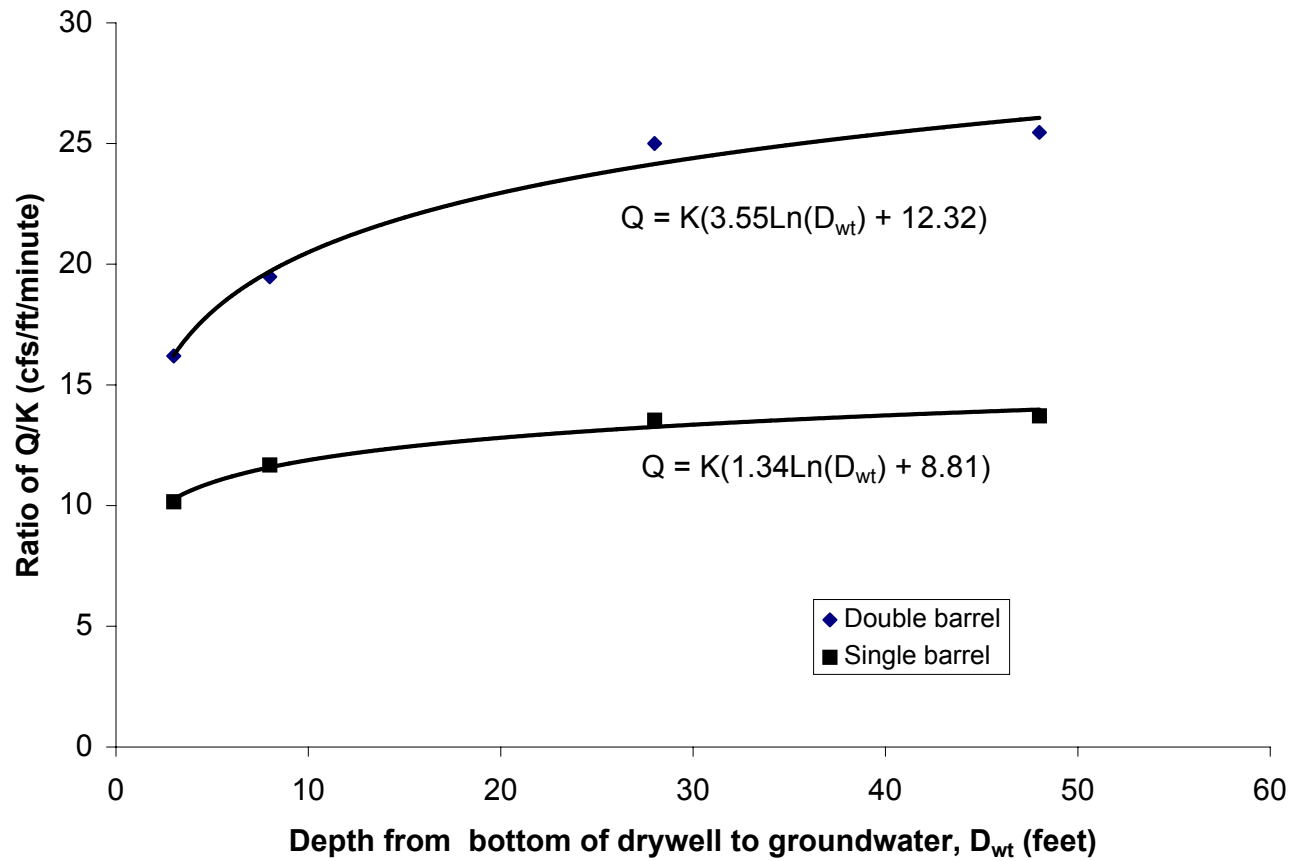


Figure 7

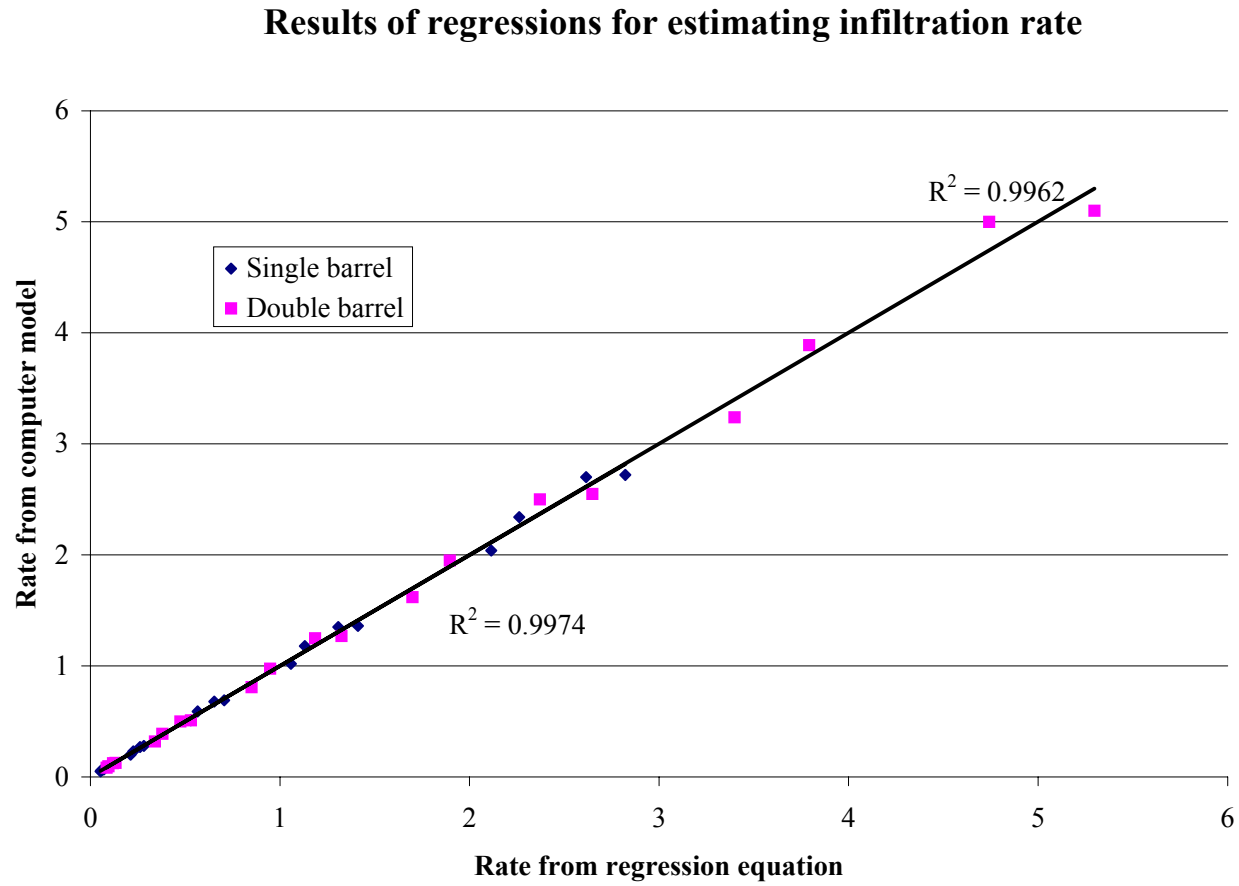


Figure 8

Observed dry well flow rates

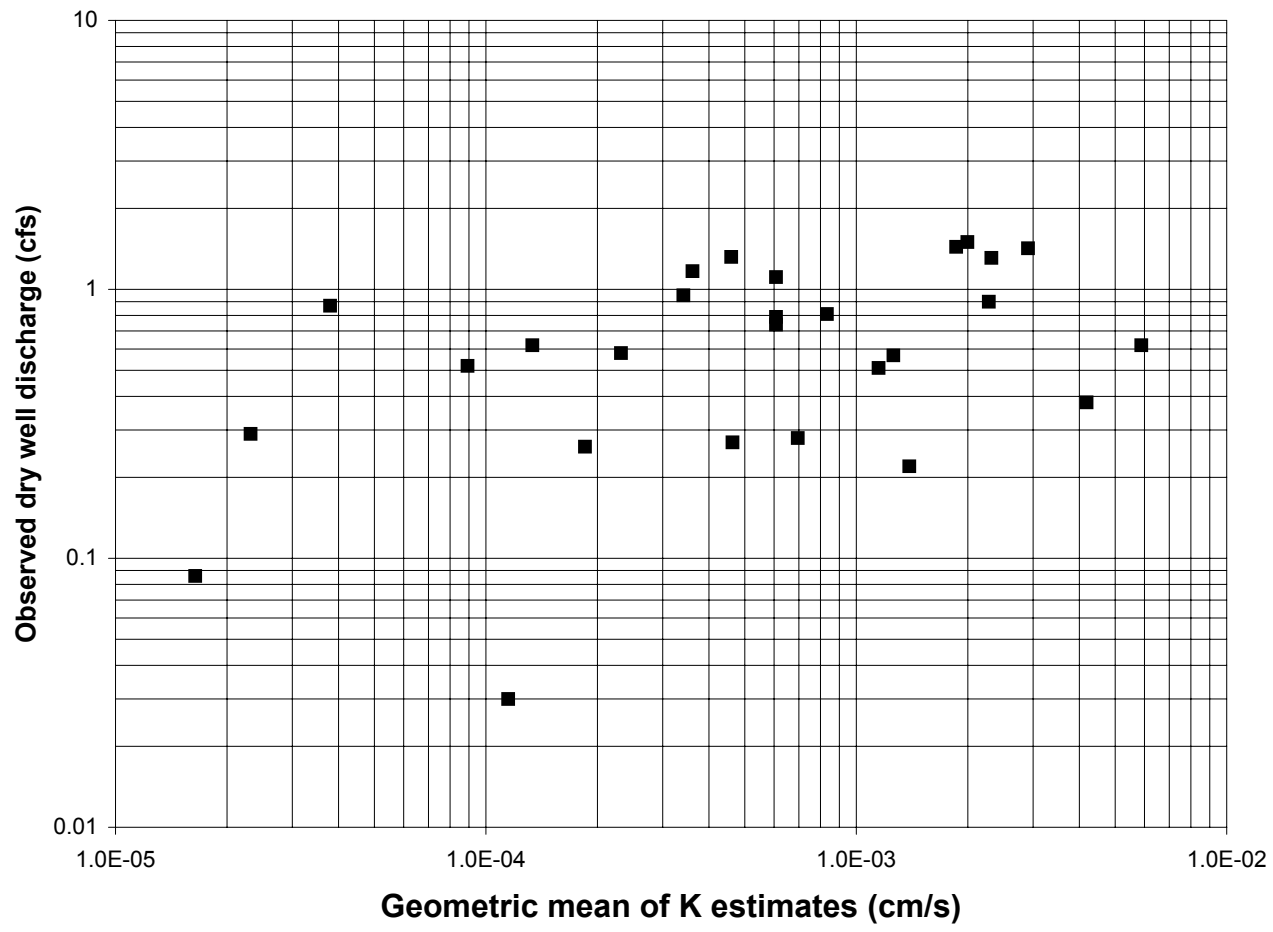


Figure 9

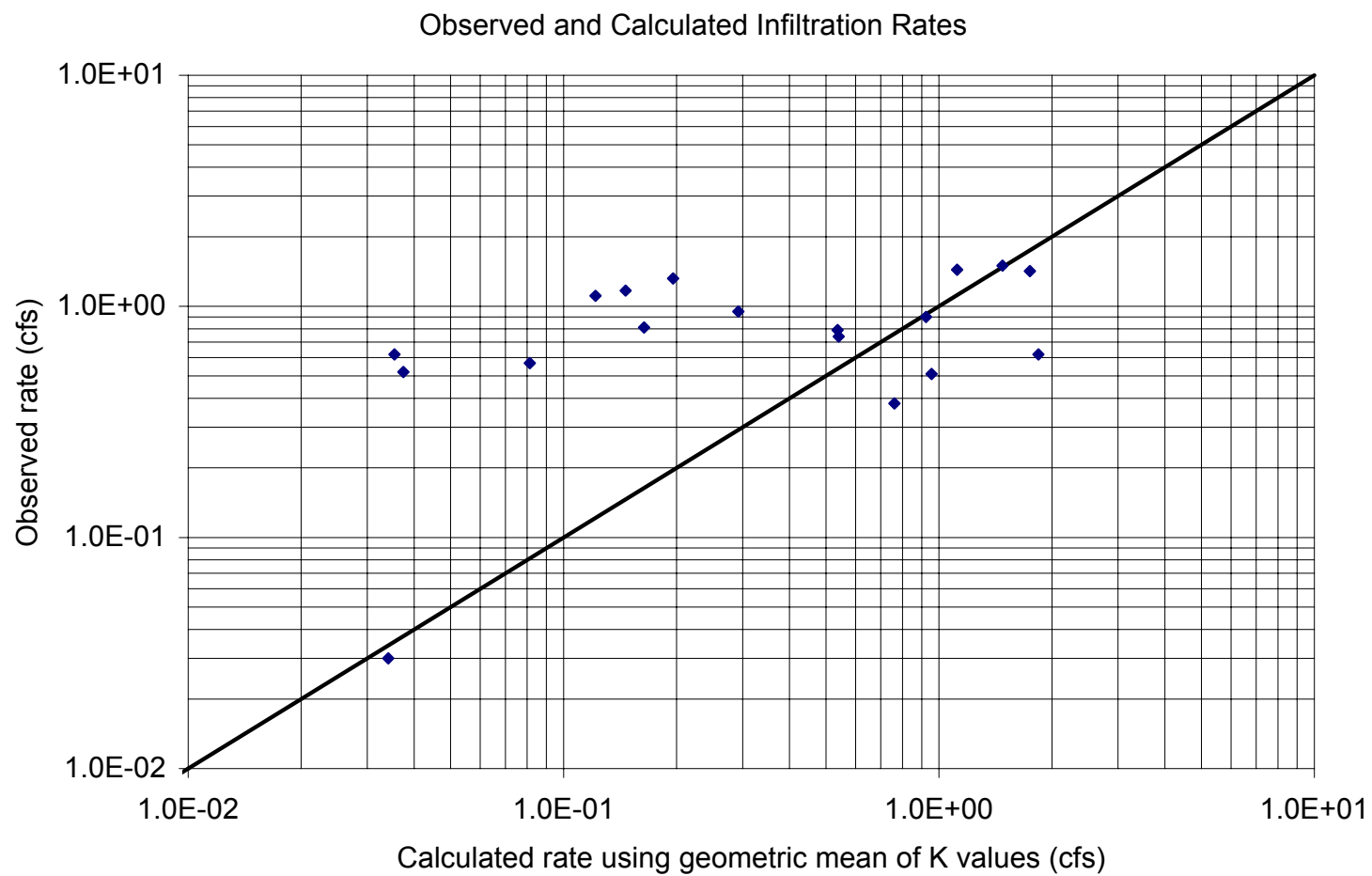


Figure 10

